JOURNAL OF MATERIALS SCIENCE 26 (1991) 1333–1345

Conversion mechanisms of a polycarbosilane precursor into an SiC-based ceramic material

E. BOUILLON*, F. LANGLAIS*, R. PAILLER*, R. NASLAIN*, F. CRUEGE‡, P. V. HUONG‡
Laboratoire de Chimie du Solide du CNRS, and ‡Laboratoire de Spectroscopie Moléculaire et Cristalline, Université de Bordeaux 1, 33405 Talence, France

J. C. SARTHOU, A. DELPUECH
CEA, Centre d'Etudes Scientifiques et Techniques d'Aquitaine, 33114 Le Barp, France

C. LAFFON, P. LAGARDE
LURE, Bt 209D, Université de Paris-Orsay, 91405 Orsay, France

M. MONTHIOUX, A. OBERLIN
Laboratoire Marcel Mathieu, Université de Pau, 2 av. du Pdt. P. Angot, 64000 Pau, France

The pyrolysis of a PCS precursor has been studied up to 1600 °C through the analysis of the gas phase and the characterization of the solid residue by thermogravimetric analysis, extended X-ray absorption fine structure, electron spectrocopy for chemical analysis, transmission electron microscopy, X-ray diffraction, Raman and Auger electron spectroscopy microanalyses, as well as electrical conductivity measurements. The pyrolysis mechanism involves three main steps: (1) an organometallic mineral transition ($550 < T_p < 800$ °C) leading to an amorphous hydrogenated solid built on tetrahedral SiC, SiO_2 and silicon oxycarbide entities, (2) a nucleation of SiC ($1000 < T_p < 1200$ °C) resulting in SiC nuclei (less than 3 nm in size) surrounded with aromatic carbon layers, and (3) a SiC grain-size coarsening ($T_p > 1400$ °C) consuming the residual amorphous phases and giving rise simultaneously to a probable evolution of SiO and CO. The formation of free carbon results in a sharp insulator–quasimetal transition with a percolation effect.

1. Introduction

Several important ceramic materials can be obtained by pyrolysis from organic or organometallic polymeric precursors. This method was first applied to carbon and then extended to a variety of refractory materials (e.g. SiC, Si_3N_4, B_4C or BN). The pyrolysis processing route has some important advantages with respect to more conventional techniques: (1) it requires lower temperatures, (2) polymeric precursors can be obtained under different states before firing (e.g. as bulk bodies, green films or fibres), (3) polymeric precursors are available with a variety of compositions as single species or as mixtures, a feature allowing the design of ceramics with specific properties [1].

In the field of composite materials, the organometallic polymer route has been widely developed for producing SiC-based fibres from a variety of organosilicon precursors, the most important contribution being that of Yajima *et al.* [2]. The processing route of the Nicalon fibre involves four steps: (1) an adjustment of the molecular weight spectrum of the polymer by distillation under vacuum or an inert gas, (2) melt spinning at about 300 °C, (3) a curing treatment by oxidation in air at about 200 °C and (4) a pyrolysis at 1200 to 1300 °C in an inert gas or under vacuum. Nicalon and related fibres have been widely studied and some correlations between their chemical nature, microstructure and mechanical behaviour have been recently suggested [3–12]. Thus, the lowering of the tensile strength of the fibres after annealing at 1200 °C has been associated with local and bulk structural features, crystallization state and chemical composition. SiC-based fibres could be described as a continuum made of SiC_4 and $SiC_{4-x}O_x$ tetrahedral species containing clusters of carbon atoms. The size of the domain of homogeneity varies from fibre grade to fibre grade and is of the order of 1 nm [13]. Both chemical and microstructural heterogeneities vary from the surface to the bulk from fibre grade to fibre grade and as function of the pyrolysis conditions. The oxygen content, silicon oxide surface layer, CO evolution, free carbon elimination as well as β-SiC grain growth are thought to be some determining factors in the thermal stability of Nicalon-type fibres.

Up to now, the mechanisms which are involved in both the synthesis of the fibres and the evolution of their behaviour during high-temperature annealing, are not well known. As far as known, the only detailed

* *Present address*: Laboratoire des Composites Thermostructaux (UM 47-CNRS-SEP-UB1), Europarc, 3 Av. Léonard de Vinci, 33600. Pessac, France.

0022–2461/91 $03.00 + .12

analysis of the successive steps of the polycarbosilane pyrolysis has been given by Yajima and his co-workers [14]. On the basis of thermogravimetric–differential thermal analysis (TGA–DTA), infrared X-ray diffraction (XRD) and chemical analysis as well as gas pressure measurements, they suggested a pyrolysis mechanism involving six steps: (1) at 20 to 350 °C, an evaporation of low molecular weight species; (2) at 350 to 550 °C, a dehydrogenation and dehydrocarbonation condensation; (3) at 550 to 850 °C, a decomposition of the side chains of the polymer giving rise to an amorphous inorganic material with a three-dimensional network; (4) at 850 to 1050 °C, end of formation of the amorphous residue; (5) at 1050 to 1300 °C, crystallization of β-SiC with a mean grain size of 2 to 3 nm, and the occurrence of free carbon and α-quartz; and finally (6) at 1300 to 1600 °C, coarsening of the α-SiC microstructure and decrease in the number of Si–O bonds.

The aim of the present study was to gain additional information on the pyrolysis of a given polycarbosilane precursor, used as a reference material, on the basis of a variety of characterization techniques either new or already used in this field.

2. Experimental procedure

The polycarbosilane (PCS, Shinetsu, Japan) used in this study was thought to have been prepared according to the Yajima's route (i.e. by thermal decomposition and condensation of polydimethylsilane at about 450 °C in an autoclave) [14–16]. Its molecular structure can thus be described, at least in a first approximation, by the theoretical formula $-[HSiCH_3–CH_2]-_n$. Its molecular weight distribution was slightly modified (i.e. the large mass fractions were eliminated by distillation).

Most pyrolysis experiments were performed in an r.f. induction furnace maintained under a pressure of 1 to 100 kPa of argon carefully purified. The apparatus has a water-cooled stainless steel jacket and a rotating sample holder equipped with a set of small alumina crucibles containing the polymeric precursor. With this device, several experiments could be successively performed, in a single run, at different pyrolysis temperatures. The most commonly used temperature–time pyrolysis conditions are given in Fig. 1. The samples were first regularly heated to a temperature T_p (slowly for $200 < T_p < 800$ °C and then more rapidly) and maintained at this temperature 0.5 to 1 h (in a few cases, the temperature plateau was as long as 20 h). From one sample to the other, T_p was increased from 500 to 2200 °C.

The analysis of the gaseous species resulting from the polycarbosilane pyrolysis was performed under very different temperature–time conditions (i.e. by flash pyrolysis). A small sample (usually 0.5 mg) was heated very rapidly, with a platinum resistor microfurnace, at a given temperature (ranging from 400 to 1000 °C) which was further maintained constant for 10 sec. The gaseous species formed during the pyrolysis were transported with a helium flow to a chromatograph (Poropak Q column) where the different

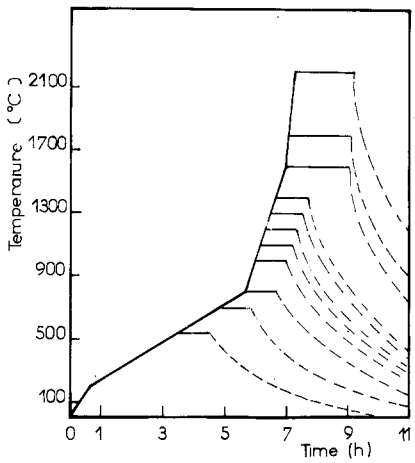

Figure 1 Various heat-treatment cycles for pyrolysis experiments.

molecules were separated. Finally, the identification of the gaseous species was performed with a mass-spectrometer coupled with a computer for the treatment of the data. The gaseous species resulting from both types of pyrolysis procedures were found to be the same. However, in the flash pyrolysis, the evolution of a given species takes place with a shift of 150 to 200 °C towards the high temperatures.

Electron spectroscopy for chemical analysis (ESCA) was performed with an X-ray microbeam, 300 μm diameter, under ultra-high vacuum (10^{-6} Pa). Auger electron spectroscopy (AES) analysis was carried out with a 250 nm probe. Both spectrometers were equipped with ion guns used to etch the sample surface. The extended X-ray absorption fine structure (EXAFS) study was performed with the ACO storage ring at LURE operated at 540 MeV and an average current of 100 mA. The Raman spectra were recorded with a 1 μm microprobe (laser wavelength 514.5 nm). The other analyses, i.e. chemical analysis, TEM, TGA, infrared, X-ray diffraction and electrical conductivity were performed according to conventional procedures.

3. Results

During the successive steps of the pyrolysis of a polycarbosilane, two kinds of phenomenon should be studied: (1) the evolution of gaseous species and (2) the transformations occurring in the condensed phase.

3.1. Analysis of the gaseous species

The chromatograms and mass spectra recorded during the flash pyrolysis of the polycarbosilane, at increasing T_p temperatures, are given in Fig. 2. The main species which have been clearly identified are alcanes (i.e. methane and ethane) and methylsilane as well as ethylene and carbon monoxide for the highest temperatures (800 to 1000 °C). Assuming that hydrogen and heavy molecules do not contribute significantly to the gas evolution (the former due to its low molecular weight, the latter to their small amount), a tentative quantitative analysis, the results of which are shown in Fig. 3, has been performed. Up to 600 °C, very little gas evolution is observed although TGA analysis,

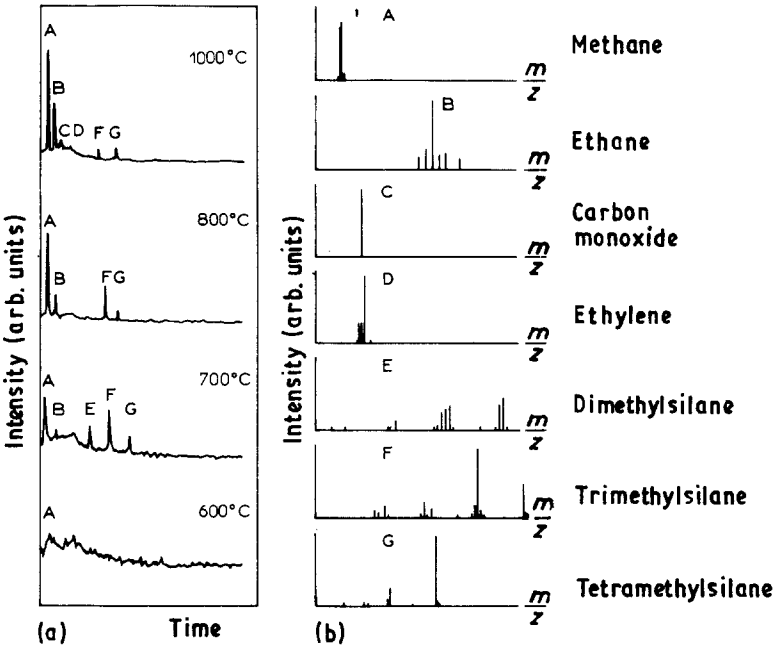

Figure 2 Identification of the gaseous species resulting from the flash pyrolysis of polycarbosilane: (a) chromatograms, (b) mass spectra (m = ion mass, z = ion charge).

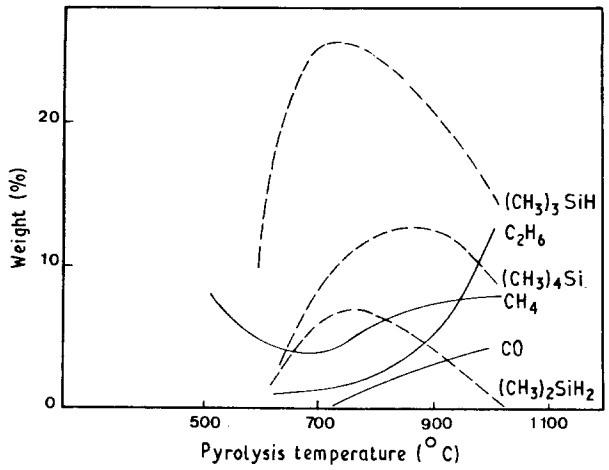

Figure 3 Tentative quantitative analysis of the gaseous species resulting from the pyrolysis of polycarbosilane as a function of temperature (the massive percentages are given with respect to the pyrolysed mass).

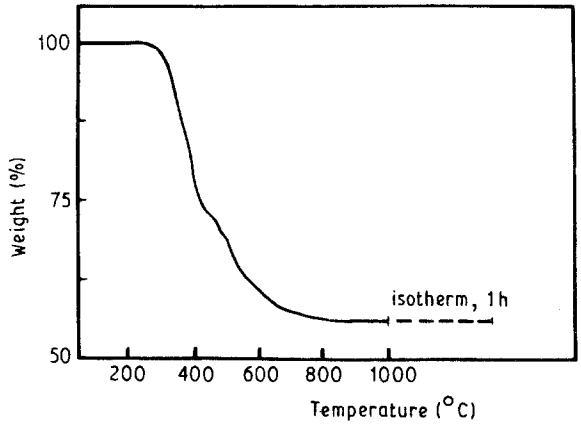

Figure 4 TGA of the weight loss observed during the pyrolysis of a polycarbosilane.

indicating already a 40% weight loss, as shown in Fig. 4, in agreement with the results previously reported by Yajima *et al.* and by Poupeau *et al.* [3, 14, 18]. Besides the shift in temperature already mentioned between pyrolyses performed conventionally (e.g. TGA) and under flash conditions, the evolution of heavy molecular weight gaseous species, easily recondensable, and corresponding to a very small gas volume hardly detectable up to 700 °C, an evolution of various methylsilanes (and to a lesser extent, light alcanes) occurs. Above about 800 °C, the relative concentrations of the gas phase in methylsilanes decrease and the light carbon-containing species (i.e. mainly CH_4 and C_2H_6) are produced preferentially. At least small amounts of carbon monoxide and hexamethylcyclotrisiloxane are identified due either to the oxygen present in the starting material (i.e. 1% to 1.5%) or to some contamination during the experiment (PCS are very sensitive to moisture and oxygen).

3.2. The organic–inorganic transition

The occurrence of an organic–inorganic transition established on the basis of the gas species analysis (the gas species result from broken organic bonds and recombination processes) is also confirmed by the infrared characterization of the condensed phases. In fact, the evolution of the infrared spectra with respect to the pyrolysis temperature (Fig. 5), is very similar to that previously reported by Yajima *et al.* [3, 14]. Up to 550 °C under conventional pyrolysis conditions (and 700 to 750 °C for flash pyrolysis), all the expected absorption peaks corresponding to the theoretical formula of the polymer are observed (i.e. C–H at 2900 and 2950 cm^{-1}; Si–H at 2100 cm^{-1}; Si–CH_3 at 1400 cm^{-1} and Si–CH_2–Si at 1355 cm^{-1}). The peak intensities decrease slowly up to T_p = 550 °C, a feature which confirms that the polymer is only weakly degraded up to this temperature, as already identified from the gas species analysis. Under such conditions only a few organic bonds are broken, resulting in the formation of low molecular weight polymers. Between 550 and 700 °C, the sbsorption bands due to the organic

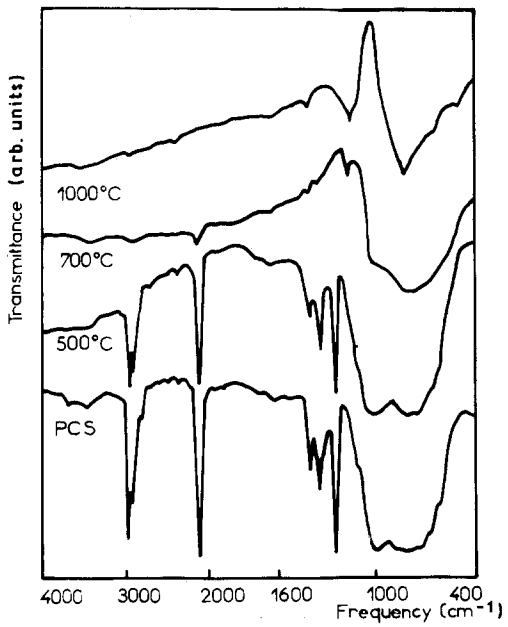

Figure 5 The organic–inorganic transition during the pyrolysis of polycarbosilane as evinced from the infrared spectra of the pyrolysis residues.

TABLE I Chemical analysis of various pyrolysis products

Pyrolysis temperature (° C)	Si (at. %)	C (at. %)	O (at. %)	H (at. %)
800[a]	31[a]	33[a]	18[a]	18[a]
1000	31	44	13	12
1400	34	52	12	2
1600	38	59	2	1

[a] At 800 °C, the results should be taken with care due to uncontrolled evolution of light hydrocarbon molecules during the analysis procedure.

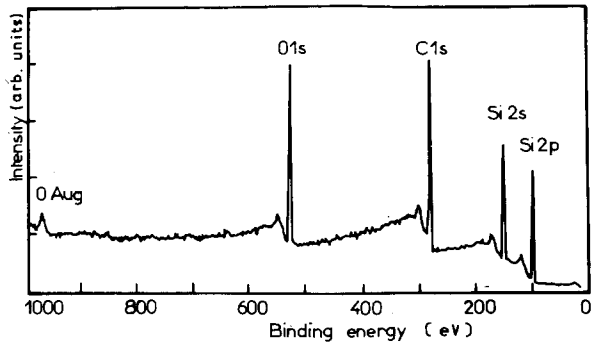

Figure 6 ESCA spectrum of the pyrolysis residue of polycarbosilane.

bonds decrease in a dramatic manner, a feature which evinces a strong degradation of the polycarbosilane. It seems reasonable to assume that the broken hydrocarbon and silane side entities form, by recombination, those species which have been identified by gas phase analysis. Above 700 °C (or 850 to 900 °C in flash pyrolysis), the infrared spectra do not change markedly, i.e. the bonds between hydrogen and carbon (or silicon) which are characteristic of the organic state are no longer detected while Si–C and Si–O large bonds (between 800 and 1100 cm^{-1}) are observed.

3.3. Chemical analysis of the pyrolysis residues

The results of chemical analyses performed on the residues resulting from pyrolyses run at increasing T_p are given in Table I. It appears that the thermal degradation of the organometallic polymer, which has been already established to be significant at 800 °C from gas analysis and TGA, is achieved only above 1000 °C, as evinced from the variation of the hydrogen concentration with temperature. As T_p is raised, both silicon and carbon concentrations increase whereas there is a marked decrease in the oxygen and hydrogen contents. Finally, at 1600 °C, the residue is almost free of oxygen and hydrogen. Thus, by assuming that SiC is stoichiometric, it appears that the final residue of the pyrolysis of the polycarbosilane is a mixture of SiC and free carbon.

The pyrolysis residues were also characterized by ESCA and AES. For all pyrolysis conditions, the ESCA spectra of the residues exhibit peaks characteristic of silicon, carbon and oxygen, as shown in Fig. 6. From the deconvolution of the Si 2p and C 1s peaks of the high-resolution spectra, a semiquantitative analysis of the chemical bonds has been tried.

The 2p silicon peak can be analysed on the basis of three components: the first, occurring for a binding energy of 100.8 eV corresponds to the Si–C bond in silicon carbide, the second at 103.5 eV is assigned, as recently suggested by several authors [13–19], to the Si–O bond in silica, and the third at an intermediate energy of 101.8 eV could be assigned to silicon atoms bound to both carbon and oxygen (Fig. 7). Similarly, the 1s carbon peak can be analysed on the basis of four components: the first at 282.8 eV corresponds to carbon bound to silicon, the second at 284.2 eV could be assigned to the oxycarbide Si(C, O) species or to free aromatic carbon (and to a lesser extent to C–H bonds) [13, 19, 20] and the other two, occurring at higher binding energy, can be attributed to carbon–oxygen bonds (i.e. C–O and C=O) (Fig. 8). Furthermore, the analysis of the 1s oxygen peak reveals a shoulder (on the high binding energy side of the peak) whose intensity increases with increasing T_p. Its assignment to a given bond is difficult because of the very low chemical shifts observed for this element. Thus, ESCA provides evidence for the occurrence in the pyrolysis residues of chemical species which are not well defined and could be regarded as species intermediate between SiC and SiO_2 (e.g. related to Si(O, C) tetrahedra). Such species, sometimes referred to as Si–X (or O–Si–C), have already been reported by Sawyer *et al.* [9] or by Lipowitz *et al.* [21] and more recently Laffon *et al.* as well as Porte and Sartre [13, 19]. The occurrence of species intermediate between SiC and SiO_2 has also been ascertained by AES analysis. As shown in Fig. 9, the *EN* (*E*) direct Auger electron spectra, recorded in the energy range corresponding to the electronic transition of silicon after ion etching of increasing duration, clearly show a fine structure with two shoulders between the 74 eV peak characteristic of silicon in

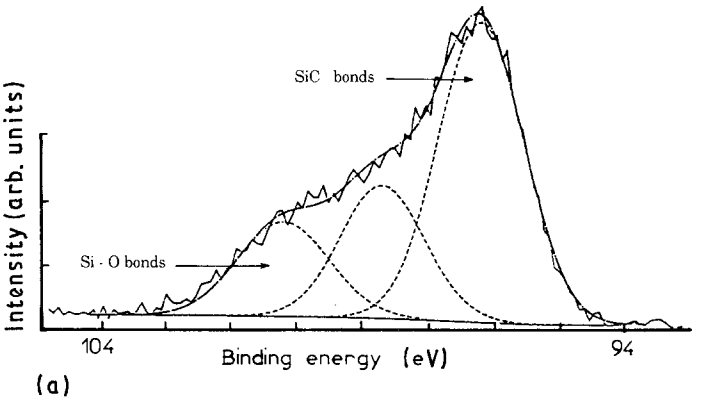

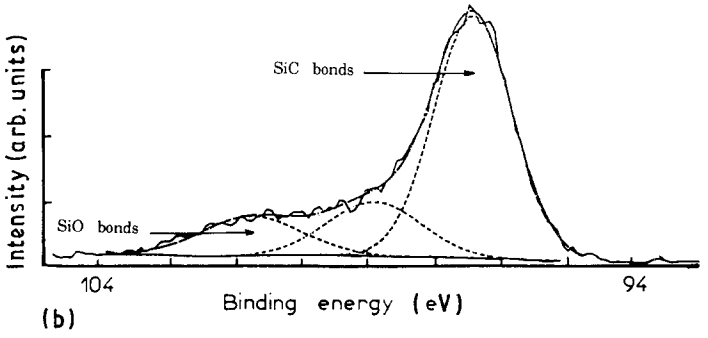

Figure 7 Deconvolution of the ESCA 2p silicon peak of pyrolysis residue: (a) $T_p = 800\,°C$; (b) $T_p = 1400\,°C$.

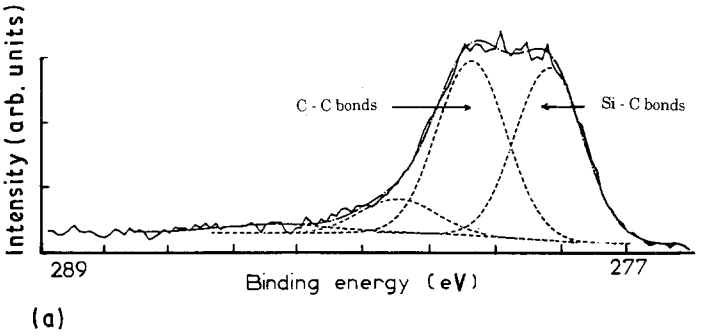

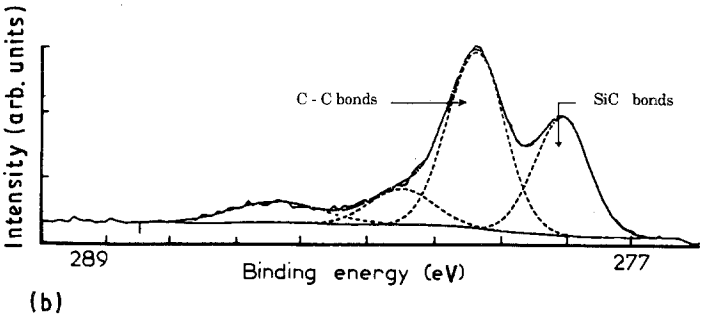

Figure 8 Deconvolution of the ESCA 1s-carbon peak of pyrolysis residue: (a) $T_p = 800\,°C$; (b) $T_p = 1400\,°C$.

SiO_2 and the 86 eV peak characteristic of silicon in SiC [22].

A semi-quantitative analysis of the chemical bonds present in the pyrolysis residues has been made from the ESCA spectra. The results for unetched samples are given in Table II. There is an acceptable agreement between the Si–C bond contents derived from the Si 2p and C 1s peaks regarding the difficulty of an accurate separation of the peak components. Moreover, the oxygen content appears to be very high, with respect to that obtained by chemical analysis of the bulk (Table I), at any T_p. Eventually, the hydrogen

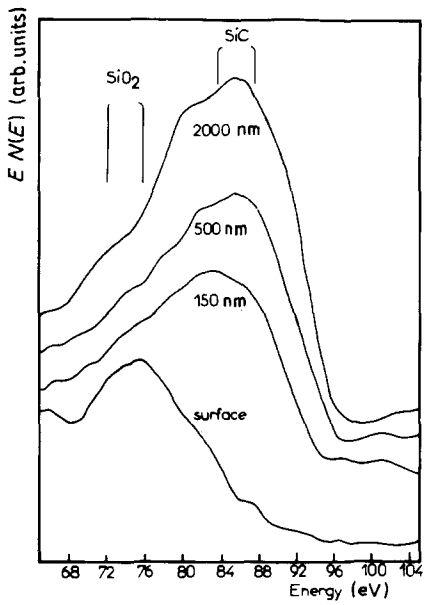

Figure 9 Auger electron peaks corresponding to the electronic transition of silicon recorded from a pyrolysis residue after etching of increasing duration.

concentration, known to be not negligble for $T_p < 1400\,°C$, need not be taken into account.

In order to study the possible occurrence of concentration gradients near the sample surface, ESCA spectra were recorded after a deep etching (i.e. 20 min ion etching) on a residue obtained at $T_p = 1400\,°C$. As shown in Table II, the ESCA semi-quantitative analysis appears to be in rather good agreement with the composition of the bulk (Table I). This is particularly true for oxygen. Furthermore, the vanishing of the high-energy components of the carbon 1s peak (assigned to both C–O and C=O bonds) suggests that part of the oxygen near the surface is present in adsorbed chemical species, such as CO_2. On the basis of the ESCA data and assuming that the species present in the residues are SiC, SiO_2, Si–X and free carbon (including carbon from the hydrocarbon compounds), the relative atomic concentrations were calculated. Their variations as a function of T_p near the sample surface and after etching are shown in Fig. 10. It is noteworthy that there is, near the surface, both a rapid increase in the free carbon content and a decrease in Si–X species as T_p is raised to about 1000 °C. Furthermore, it appears, from the data obtained on the sample etched at 1400 °C, that the content in free carbon is much higher near the sample surface than in the bulk and that it is the reverse for Si–X. These results are in agreement with the occurrence of a carbon-rich thin layer often found around Nicalon-type fibres annealed at high temperatures and support the hypothesis that it could result from the thermal decomposition of a ternary Si(C, O) phase.

3.4. Microstructural analysis of the pyrolysis residues

The solids resulting from the pyrolysis of polycarbosilane are amorphous for $T_p < 1000\,°C$ as shown by X-ray diffraction analysis (Fig. 11). Above this temperature, broad diffraction peaks corresponding to β-SiC are observed. Assuming that the pyrolysis residues are not microstrained, the line-broadening effect (i.e. the Scherrer equation) has been used to assess the mean grain size. As illustrated in Fig. 11 the diffraction peaks become sharper and sharper as T_p increases, suggesting a progressive crystallization process. The variations of the apparent grain size as a function of T_p are shown in Fig. 12. Up to $T_p = 1400\,°C$, the apparent grain size increases slowly and remains smaller than about 5 nm, then it undergoes an important increase (i.e. at 1600 °C, the mean grain size is of the order of 50 nm). The kinetics of growth of β-SiC have been roughly estimated by plotting the variations of the mean apparent grain size as function of the duration of the T_p plateau (from 1 to 20 h) (Fig. 13). At a given temperature, the apparent grain size increases rapidly during the first 2 h, then very slowly.

The short-range order around silicon has been investigated by EXAFS experiments carried out on the Si*K* edge. The samples resulting from pyrolyses performed at T_p ranging from 800 to 1600 °C were reduced to powders (mean particle size less than 1 μm) and deposited on a membrane as a thin film for experiments in the transmission mode. Amorphous silica and crystalline β-SiC were used as standards for quantitative analysis. For $T_p = 800$ to 1000 °C, the residues resulting from the pyrolysis of PCS do not exhibit a defined structure beyond 0.3 nm (Fig. 14a). It is interesting to notice that the short-range order around silicon is limited, as it is in the PCS precursor,

TABLE II Analysis of the chemical bonds of various unetched pyrolysis products from ESCA experiments (the result corresponding to an etched sample obtained at 1400 °C is given for the purpose of comparison)

Pyrolysis temperature (°C)	Si (at. %)			C (at. %)				O (at. %)
	Si–C	Si–X	Si–O	C–Si	C–C, C–H	"C–O"	"C=O"	
800		26.8			42.3			30.9
	15.1	6.6	5.1	18.3	18.5	4.0	1.5	
1000		27.0			47.0			26.0
	17.0	4.8	5.2	17.8	24.2	3.8	1.2	
1200		25.9			48.2			25.9
	16.8	4.6	4.5	16.2	24.5	5.3	2.2	
1400		25.8			49.9			24.3
	17.5	4.6	3.7	15.4	25.6	4.7	4.2	
1400 after etching		39.9			47.5			12.6
	28.7	8.3	2.9	23.6	19.9	4.0		

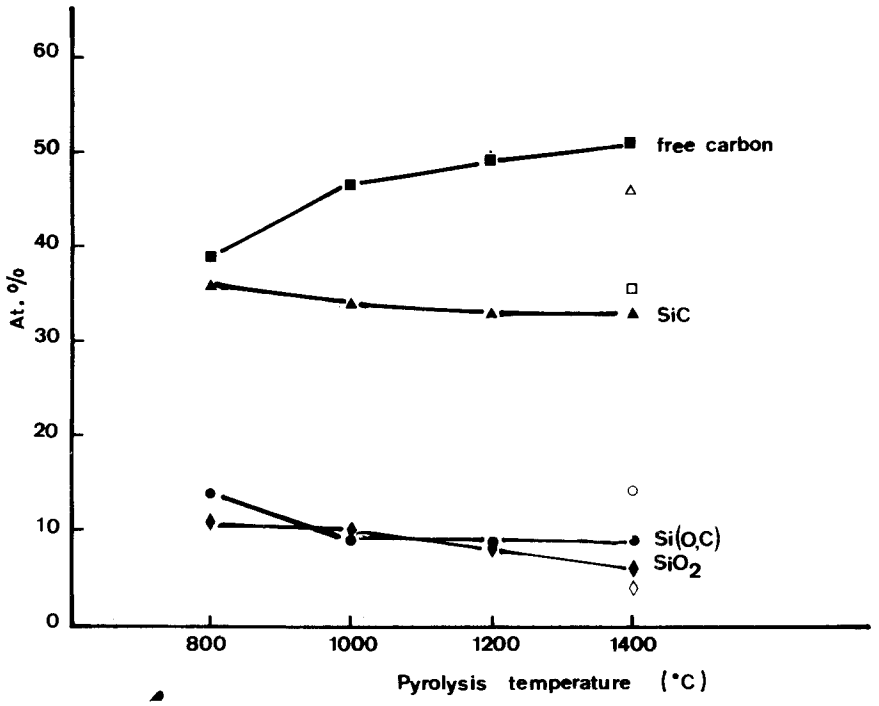

Figure 10 Variations of the atomic concentrations of the various species present in the residues as a function of the pyrolysis temperature (■, ▲, ◆, ●) before etching, (□, △, ◇, ○) after etching.

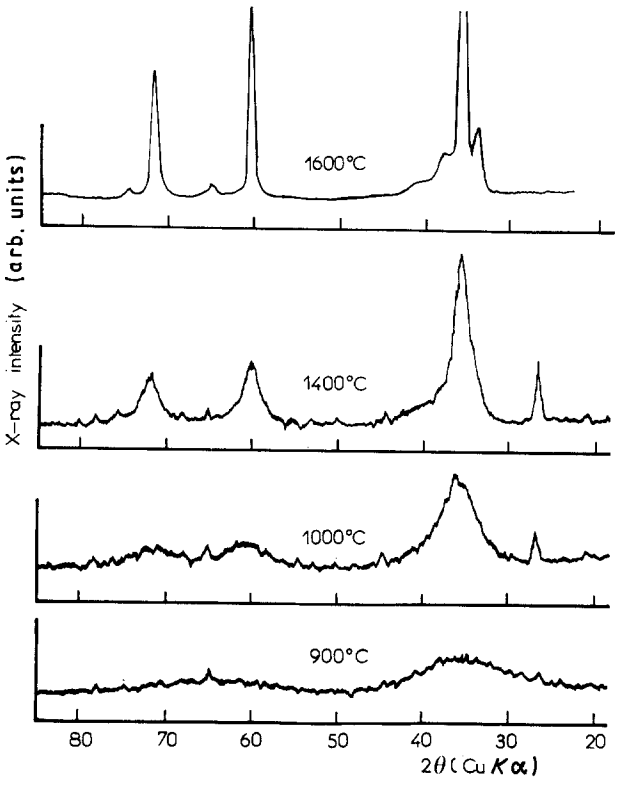

Figure 11 X-ray diffraction patterns of the solids resulting from the pyrolysis of polycarbosilane with increasing temperatures.

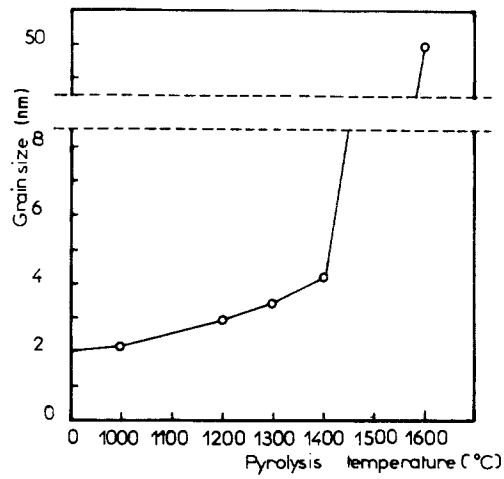

Figure 12 Variations of the mean grain size of β-SiC in the solids resulting from the pyrolysis of polycarbosilane as a function of the pyrolysis temperature.

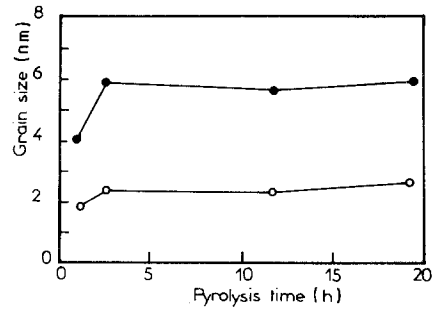

Figure 13 Kinetics of growth of β-SiC grain size in the solids resulting from the pyrolysis of polycarbosilane at (●) 1400 °C, (○) 1000 °C.

to the first shell (which corresponds to both tetrahedral Si–C and Si–O distances) and to the second shell (associated with Si–Si distances found in both crystalline SiC and amorphous silica). Thus, a memory effect during the organic–inorganic transition occurs. A similar conclusion was drawn by Laffon *et al.* for the Nicalon NLP grade fibre [13]. Furthermore, in all the samples obtained at $T_p > 1200\,°C$, a crystalline ordering occurs which extends well beyond 1.5 nm (Fig. 14b). This crystallized ordering is very close to that of β-SiC but additionally some atomic surrounding typical of that present in amorphous silica is always observed. The amount of silica is found to decrease from about 13% to 7% with increasing T_p.

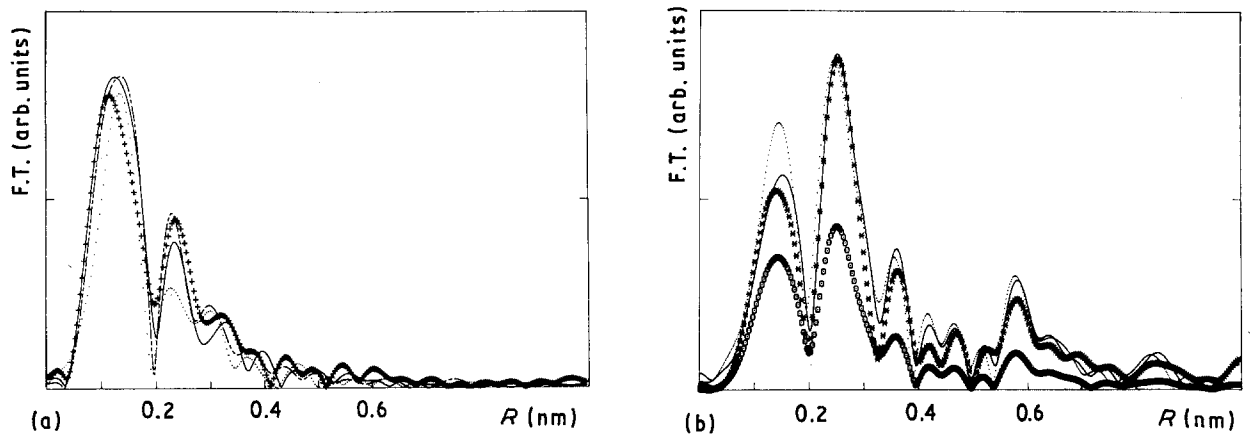

Figure 14 EXAFS analysis (a) of the materials resulting from the pyrolysis of (···) PCS at (——) 800 °C, and (+) 1000 °C, and (– – –) PCS cured in air at 170 °C; and (b) of the ceramics (*) obtained by pyrolysis at (——) 1600 °C, (···) 1400 °C, (○ ○ ○) 1200 °C.

From the EXAFS data, the ceramization threshold (i.e. the transition from the amorphous state to a crystalline material) has been estimated to lie between 1000 and 1200 °C.

Raman microprobe has been used, rather recently, to characterize pyrolytic carbon [23–26] as well as CVD thin films of amorphous silicon carbide [27–29] or SiC-based CVD filaments [30]. According to Lespade *et al.* [23] the graphitization of carbons can be followed through the variations of four indices: the wave number and width of the E_{2g} line (1580 to 1600 cm^{-1}) which characterizes the extent of the two-dimensional graphitic domains, the occurrence of a 1350 cm^{-1} line due to lattice defects and the width of the 2700 cm^{-1} line (second order) which permits the final stage of the graphitization process (tridimensional ordering) to be followed. Amorphous silicon carbide films give rise to three groups of bands corresponding to Si–Si, Si–C and C–C bonds [28]. Even when containing low percentages of free carbon, the intensity of the C–C band (1300 to 1600 cm^{-1}) in the films is much higher than those related to the Si–Si band (300 to 600 cm^{-1}) and the Si–C band (700 to 1000 cm^{-1}) due to a better Raman efficiency. As a result, Raman analysis was preferentially used to structurally characterize the free carbon in the films. Only a few studies have been carried out in the field of the ordering state of SiC itself. Two lines are usually observed at 789 and 967 cm^{-1} assigned to the cubic low-temperature β-modification, the former being often stronger than the latter as reported by Martineau *et al.* for SiC CVD filaments [30].

Raman microprobe analyses were performed on the residues obtained under different pyrolysis conditions with the following main features: (1) the presence of free carbon in all the samples, (2) a better definition of the SiC lines as T_p is increased and (3) the occurrence of heterogeneities (in both concentration and crystallization state) within the samples. Some of the most representative Raman spectra corresponding to increasing T_p are shown in Fig. 15. As far as free carbon is concerned, a single broad asymmetric band at about 1500 cm^{-1} is observed for $T_p = 850$ °C, suggesting that carbon is totally amorphous or still bound to hydrogen atoms [28]. The splitting of this band,

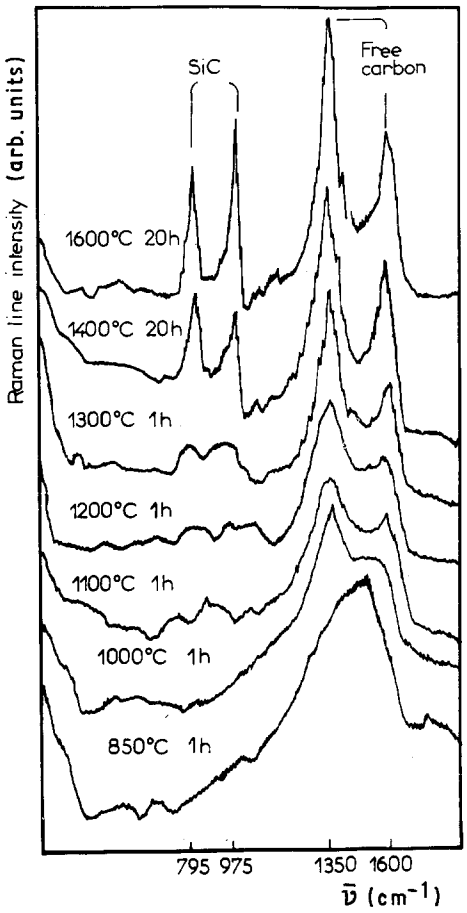

Figure 15 Evolution with T_p of the Raman spectra of the residues resulting from the pyrolysis of PCS.

which begins at 1000 °C (giving rise to the classical 1580 and 1350 cm^{-1} lines), evinces the formation of true free carbon. Then the Raman spectrum of carbon does not change markedly up to 1600 °C (with the exception of a progressive narrowing of the lines). Finally, above 1800 °C, the respective intensities of the two lines reverse (e.g. at 2200 °C the one at the 1350 cm^{-1} line is much lower) suggesting an evolution of the free carbon towards carbon crystallites of larger size (Fig. 16). Similarly, the Raman lines characteristic of crystalline SiC are almost unobservable for the lowest T_p values (Fig. 15). On the contrary, for

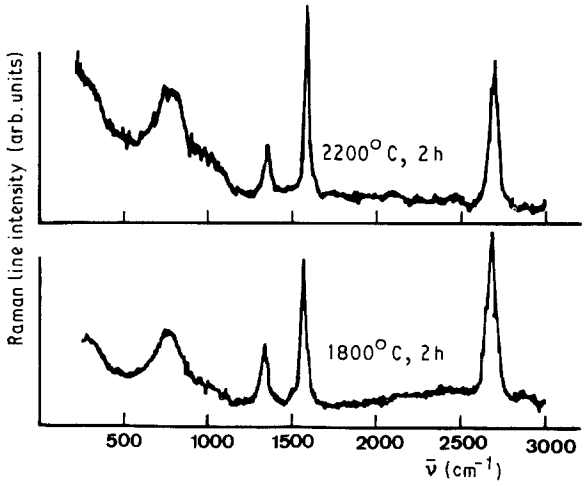

Figure 16 Raman spectra of the residues resulting from the high-temperature pyrolysis of PCS.

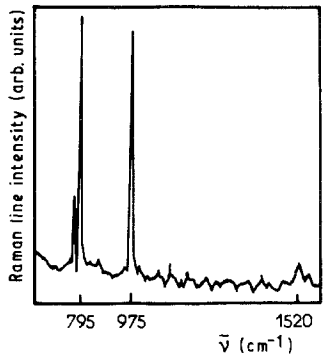

Figure 17 Raman spectrum of the high-temperature modification of SiC.

$T_p > 1200\,°C$ two broad lines occur at about 795 and 975 cm^{-1} becoming sharper as T_p increases, due to a better crystallization state. As can be seen in Figs 15 and 17, the spectrum definition was not good enough, even for $T_p = 1600\,°C$, to ascertain the occurrence of a small amount of α-SiC (whose higher lattice symmetry results in a third Raman line of low intensity at 780 cm^{-1}).

In order to confirm the occurrence of chemical and structural heterogeneity within the residues resulting from PCS pyrolysis, already partly established by ESCA, point analyses (made possible by the space resolution of Raman microprobe) were performed on a cross-section. Due to the high Raman efficiency of the C–C bonds (which give lines of high intensity even for low carbon concentrations), it has not been possible to observe any heterogeneity in the free carbon distribution. On the contrary, the crystallization state of SiC within residues obtained at $T_p = 1400\,°C$ was found to be dependent upon the analysed area, i.e. both 789 and 967 cm^{-1} lines exhibit variable intensities and even totally vanish. For $T_p = 1600\,°C$, the heterogeneity of the residues seems to be less significant, the SiC lines being always observed whatever is the analysed area.

The PCS pyrolysis residues were also analysed by transmission electron microscopy (bright-field, dark-field, high-resolution lattice fringes, selected-area electronic diffraction). The results of this detailed analysis will be reported elsewhere and are only summarized here for the purpose of the discussion [31]. The heterogeneity of the pyrolysis residues discussed above is confirmed by the results of the TEM analyses carried out on crushed samples except for those resulting from pyrolyses performed at $T_p < 850\,°C$. As an example, the material resulting from pyrolysis at 1400 °C contains the four kinds of particles which can be seen in the micrographs of Fig. 18. For $T_p < 850\,°C$, the pyrolysis residue appears to be a SiC-based amorphous phase in which it is impossible to ascertain whether free carbon or silica are present. For $T_p = 1000\,°C$, this amorphous phase (which corresponds to particle 4 in Fig. 18a) gives rise partly to a microcrystalline phase containing SiC crystals 3 nm in size (such as particle 3) and to a lesser extent to crystals 10 nm in size (corresponding to particle 2). Finally, for $T_p = 1400\,°C$, the residues exhibit a more pronounced microstructural heterogeneity with "large" crystals (about 15 nm in size, particle 1) and smaller ones which are surrounded by thin films of aromatic carbon (observed on dark-field, Fig. 18c, and lattice-fringe imaging), resulting in a sponge-like microtexture. The above results are in rather good agreement with the apparent grain size values calculated from X-ray diffraction patterns (the small difference being due to the fact that the latter are mean values while the former are measured on individual grains). On the basis of the TEM-analysis, the crystallization threshold of the pyrolysis residues of PCS, already established by EXAFS to be in the 1000 to 1200 °C temperature range, rather occurs at 1000 °C.

3.5. Electrical properties of the pyrolysis residues of PCS

The variations of the electronic conductivity appear to be a very sensitive way to follow the transition taking place between the PCS precursor and the SiC-based ceramic material by pyrolysis at increasing T_p. Conductivity measurements have been performed, according to the four-contact method, on PCS pyrolysis residues obtained at T_p ranging from 700 to 1600 °C. Nicalon fibres (NLP 101 grade) as well as polycrystalline and monocrystalline SiC were used as standards. For each sample, the variations of the electrical conductivity between 20 and 600 °C are plotted as a function of the reciprocal temperature on a semi-logarithmic scale in Fig. 19. Because the data follow Arrhenius laws, activation energies characterizing the conduction mechanism have been derived from the slopes of the straight lines. The reversibility of the electrical behaviour has been verified for all samples, a feature which indicates that the materials are stable up to 600 °C and exhibit an electronic-type conductivity. The variations of the activation energy as well as those of the conductivity at 20 °C as a function of T_p are given in Fig. 20.

For $T_p < 1000\,°C$, the pyrolysis residues are insulating materials with a conductivity lower than $10^{-10}\,\Omega^{-1}\,cm^{-1}$ at 20 °C and an apparent activation energy of 0.7 eV. The low conductivity could be due

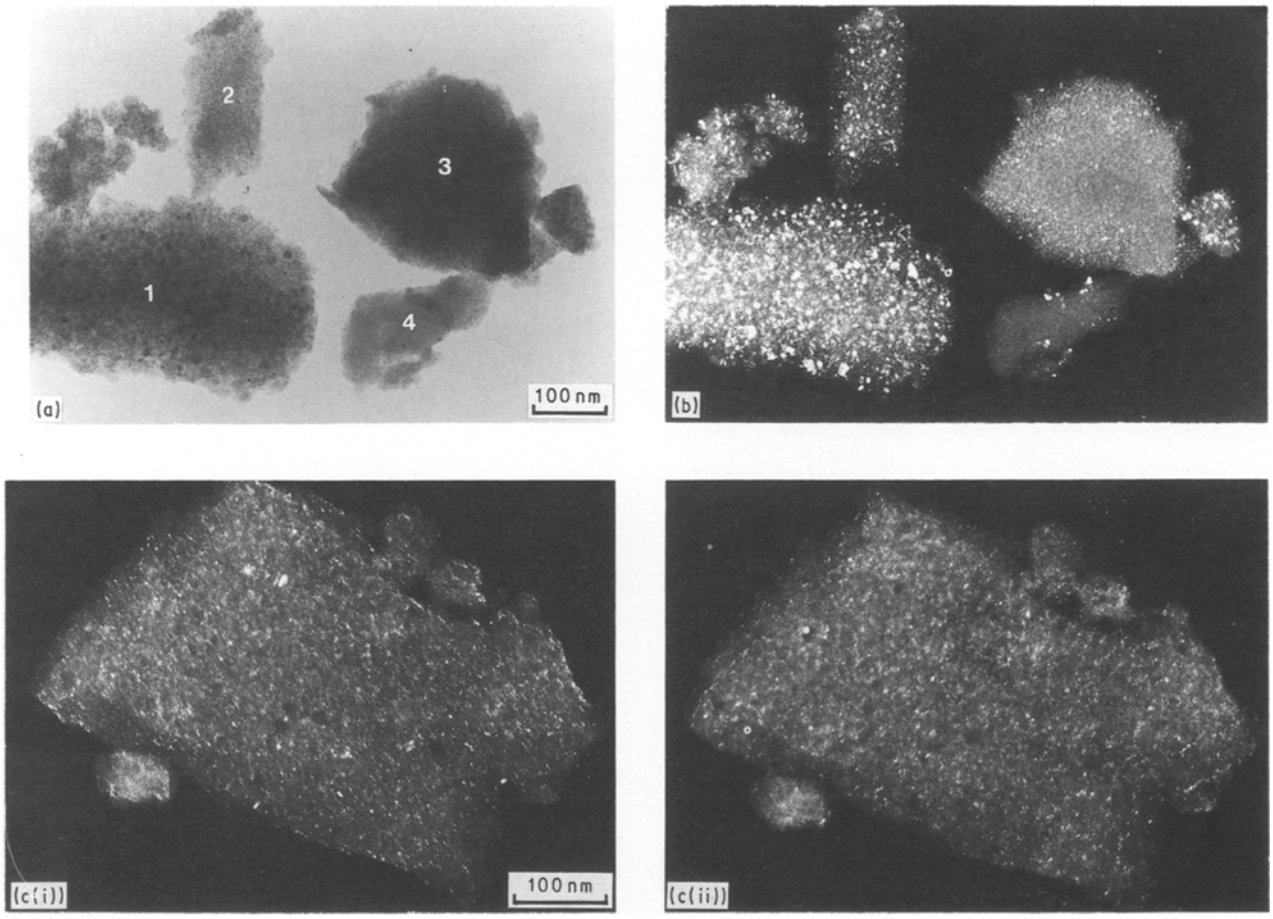

Figure 18 TEM analysis of residues resulting from PCS pyrolysis: (a) bright-field, (b) dark-field showing SiC microcrystals, (c) dark-field in two orthogonal positions showing carbon distribution.

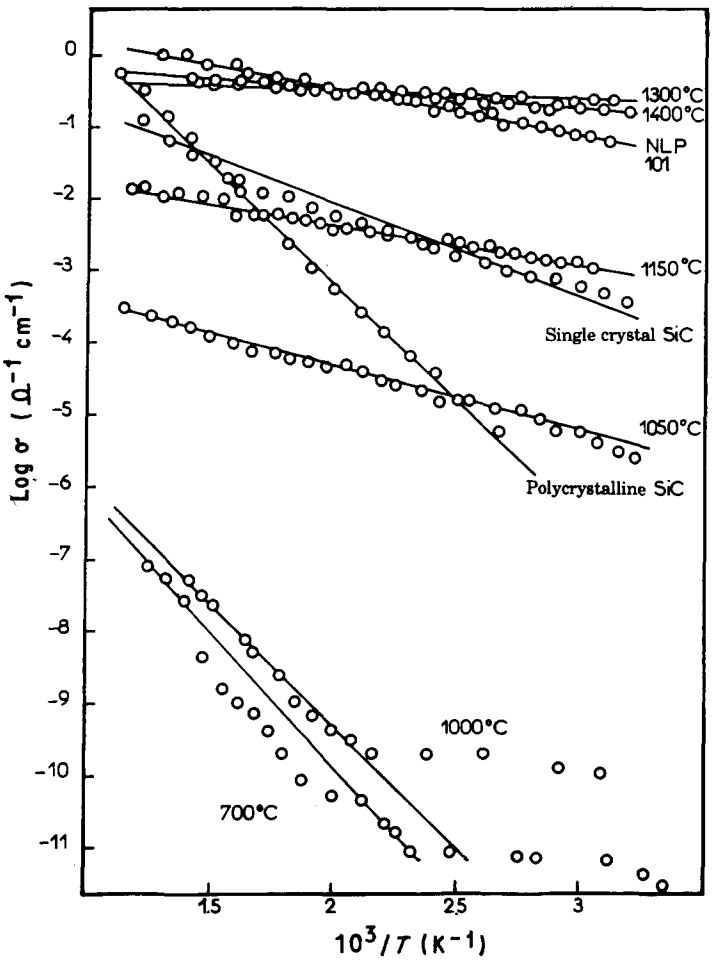

Figure 19 Temperature dependence of the electrical conductivity of materials resulting from the pyrolysis of PCS precursors.

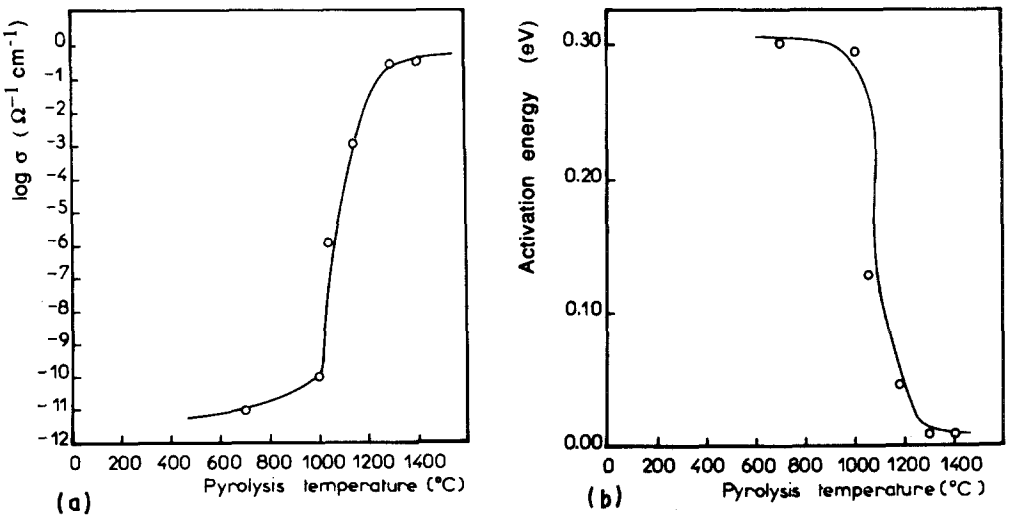

Figure 20 Variation, as a function of the pyrolysis temperature, T_p, of (a) the electrical conductivity at 20 °C, and (b) the activation energy.

either to a low mobility or a low concentration of charge carriers. For $900 < T_p < 1200$ °C, the electrical conductivity undergoes a dramatic variation, i.e. the ambient conductivity increases by a factor of ten orders of magnitude and the activation energy decreases to values lower than 0.01 eV. Finally, for $T_p > 1200$ °C, the electrical characteristics remain almost constant, the ambient conductivity being close to 1 Ω^{-1} cm^{-1} and the activation energy almost zero, a feature which suggests a partly metallic behaviour as in the related case of Nicalon fibres. On the contrary, crystalline SiC exhibits properties which are intermediate between those of residues resulting from PCS pyrolysis performed at high or low temperatures.

The evolution of the electrical behaviour of the PCS pyrolysis residues with respect to T_p has some similarity with that reported for the pyrolysis of hydrocarbon polymers into pyrocarbons. Such a process can be explained, for instance, on the basis of the following mechanism [32–33]: (1) for $T_p < 600$ °C, volatile species (e.g. CH_4) give rise to aggregates of sp^2 aromatic carbons bound to free radicals with single electron; (2) for $600 < T_p < 1200$ °C, the radicals capture the electrons of the aromatic network and leave corresponding holes which results in a rapid increase of conductivity as T_p is raised, a marked decrease in the activation energy and simultaneously an extension of the aromatic carbon domains as well as a strong decrease in the hydrogen content; (3) finally, for $T_p > 1200$ °C, the carbons (which are no longer bound to any hydrogen atoms) undergo no further change in their crystallization state up to the graphitization temperature.

In the case of the pyrolysis of PCS, the insulator–quasimetal transition occurs at a slightly higher temperature (i.e. between 1000 and 1200 °C). Regarding the semiconducting behaviour of crystalline SiC, the transition could be explained by both a segregation of free carbon at the external surface of the SiC particles and an increase in the carbon concentration on increasing T_p, which induces a percolation effect [34]. This effect seems to take place at about $T_p = 1100$ °C. This outstanding behaviour is entirely consistent with the results of all the chemical analyses reported above, concerning the amount and microstructural state of free carbon (ESCA, Raman spectroscopy and TEM).

4. Discussion and conclusion

The large variety of chemical and microstructural analyses all performed on residues resulting from the pyrolysis of the same PCS precursor has permitted, on the one hand, an increase in our knowledge of the different stages occurring during the transformation process of PCS into SiC-based ceramic materials and, on the other hand, the suggestion of a general procedure for studying other similar transitions that take place between organometallic precursors and ceramics.

Three fundamental steps occur during the pyrolysis of PCS: (1) the organometallic–mineral transition (at $550 < T_p < 800$ °C); (2) the crystallization threshold of the amorphous residue (at $1000 < T_p < 1200$ °C); and (3) a grain coarsening above 1400 °C. The intermediate steps (i.e. for $800 < T_p < 1000$ °C and $1200 < T_p < 1400$ °C) correspond to more limited changes in the composition or microstructure of the pyrolysis residues.

The experimental results which have been presented above support the following pyrolysis mechanism for the PCS precursor which has been studied here (and which is close to those used for the synthesis of Nicalon-type fibres).

(a) For $20 < T_p < 550$ °C, the structure of the polymer precursor does not change markedly as evinced from infrared analysis. Lateral organic functions do not seem to be broken significantly as shown by the gas phase analysis (i.e. absence of light gaseous species). The only important phenomenon which occurs within this temperature range is the evolution of heavy gaseous products corresponding to polymers of low molecular weight, which results in a large weight loss as established from the TGA analysis. At this stage, the polymer becomes infusible, probably due to an increase in the reticulation degree resulting from (i) the

effect of temperature, and (ii) some accidental addition of oxygen taken from the atmosphere of the pyrolysis furnace.

(b) For $550 < T_p < 800\,^{\circ}C$, the main part of the organometallic–mineral transition is effective. Most of the Si–H and C–H bonds are broken, as shown by the infrared analysis. The tetrahedral environment of silicon as well as the polymer Si–C skeleton are probably maintained (i.e. the short-range atomic order) as suggested by the EXAFS results. An important evolution of gaseous species is observed mainly consisting of light hydrocarbon molecules (i.e. CH_4, C_2H_6, . . .) and methylsilanes (i.e. $(CH_3)_4Si$, $(CH_3)_3SiH$, $(CH_3)_2SiH_2$) resulting respectively from the broken lateral chains and chain ends, as well as probably a large amount of hydrogen (which has not been analysed).

(c) For $800 < T_p < 1000\,^{\circ}C$, the material is essentially mineral but still contains some hydrogen which may have a role to play during the ceramization process. The pyrolysis residues must be regarded as homogeneous, being totally amorphous. It can be described on the basis of three chemical tetrahedral entities: (1) hydrogenated amorphous silicon carbide (including some residual hydrocarbon groupments (e.g. CH, CH_2, CH_3); (2) hydrogenated amorphous silicon oxycarbide; and (3) amorphous silica, the former being widely predominant in the bulk. As T_p increases up to 1000 °C, the hydrogen content decreases, the free carbon percentage rises, the SiX oxycarbide amount decreases and the following phenomena are thought to occur: (1) volatile hydrocarbon molecules (e.g. CH_4, C_2H_6, . . .) resulting from breaking of Si–C bonds are decomposed *in situ* instead of being evolved, when their cracking temperature is reached, i.e. probably when T_p is close to 1000 °C; (2) this decomposition proceeds at a microscopic scale (e.g. in the microvoids of the residue or near the surface) giving rise to both a few nuclei of crystalline SiC and the heterogeneity of composition which has been evinced by ESCA and TEM analyses. The insulating electrical behaviour of the material obtained within this temperature range could be attributed either to a low mobility of the charge carriers if the Fermi level lies close to localized states or to a low charge carrier concentration if the Fermi level is close to narrow bands. Finally, the evolution of a small amount of light species (e.g. silanes or carbon monoxide) could be related to a partial decomposition of the amorphous hydrogenated silicon oxycarbide whose concentration decreases (according to Johnson *et al.* SiO remains the main gaseous species resulting from the heat-treatment of ex-PCS Nicalon fibres in the 1100 to 1400 °C temperature range [35]).

(d) For $1000 < T_p < 1200\,^{\circ}C$, the number of SiC nuclei (less than 3 nm in size), which was very low at $T_p = 1000\,^{\circ}C$, notably increases while their mean size is little changed. This nucleation of SiC in the overall material becomes detectable by EXAFS (which shows, for $T_p = 1200\,^{\circ}C$, a radial distribution function around silicon well defined beyond 1 nm). As the hydrogen content decreases, hydrogenated amorphous SiC vanishes, the only residual amorphous phases being both silica (when present) and silicon oxycarbide whose stoichiometry is very difficult to determine (from the ESCA chemical shifts between SiC and SiO_2, a tentative formula for the intermediate tetrahedra could be close to SiC_3O). As SiC nuclei grow from the amorphous medium, the free carbon content slowly increases, leading to a heterogeneous material with an extremely divided microtexture: SiC nuclei are thought to be surrounded with a thin film of aromatic carbon arranged as a stack of a few layers. As a consequence of the sufficiently high free carbon concentration, the electrical properties of the material undergo a sharp insulating–quasimetallic behaviour transition according to a percolation mechanism from a concentration threshold.

(e) For $1200 < T_p < 1400\,^{\circ}C$, as the last hydrogen atoms are removed, a slow continuous crystallization of SiC is observed, the mean grain size reaching a value of about 10 nm. Simultaneously, the percentage of silica or Si(C, O) species decreases slowly (possibly due to an evolution of SiO) while the percentage of free carbon slightly rises. However, free carbon remains aromatic and the overall electrical behaviour is quasimetallic.

(f) For $1400 < T_p < 1600\,^{\circ}C$, a marked grain coarsening of the SiC microstructure is observed (the average grain size reaching a value higher than 50 nm). Simultaneously, a rapid decrease in both the amorphous silica (or silicon oxycarbide) contents occur with a probable evolution of silicon and carbon monoxides.

In summary, the various steps taking place during the pyrolysis of PCS precursor have been investigated. Interestingly, a correlation between a macroscopic behaviour, i.e. the insulator–metal transition, and a microscopic scale change, i.e. the amorphous–microcrystalline state transition related to chemical composition, has been pointed out for the first time in this field. The former, which requires simple experimental procedures, could be applied in the future to a variety of similar precursors while the latter, which supposes the use of heavy analytical techniques (e.g. TEM, EXAFS, . . .), could be better limited to the detailed study of a few chosen organometallic polymers.

Acknowledgements

This article is the result of a cooperative research programme which has been supported by SEP, the French Ministry of Defence (DRET), CNRS, CEFI, AFME and Conseil Régional d'Aquitaine. The authors acknowledge the contributions of Dr J. Dunogues, E. Bacqué, J. P. Pillot and M. Birot (CNRS-UA 35) for the supply of the PCS precursor and assistance in understanding different problems related to organometallic chemistry, P. Orly (SEP) for help in interpreting the structure of the pyrolysis residues, E. Marquestaud for the conductivity measurements, J. J. Videau for infrared recording and M. Lahaye for the AES analyses. The ESCA analyses were performed by A. Sartre from Science et Surface Co.

References

1. R. W. RICE, *Ceram. Bull.* **62** (1983) 889.
2. S. YAJIMA, in "Handbook of Composites", Vol. 1, "Strong Fibers", edited by W. Watt and B. V. Perov (Elsevier Science, New York, 1985) p. 201.
3. Y. HASEGAWA, M. IIMURA and S. YAJIMA, *J. Mater. Sci.* **15** (1980) 720.
4. T. MAH, N. L. HECHT, D. E. McCALLUM, J. R. HOENIGMAN, H. M. KIM, A. P. KATZ and H. A. LIPSITT, *ibid.* **19** (1984) 1191.
5. G. SIMON and A. R. BUNSELL, *ibid.* **19** (1984) 3649.
6. *Idem., ibid.* **19** (1984) 3658.
7. T. J. CLARK, R. ARONS, J. RABE and J. B. STAMATOFF, *Ceram. Engng Sci. Proc.* **6** (1985) 576.
8. T. J. CLARK, M. JAFFE, J. RABE and N. R. LANGLEY, *ibid.* **7** (1986) 901.
9. L. C. SAWYER, R. T. CHIN, F. HAIMBACK, P. J. HARGET, E. R. PRACK and M. JAFFE, *ibid.* **7** (1986) 914.
10. K. OKAMURA, *Composites* **18** (1987) 107.
11. A. S. FAREED, P. FANG, J. KOCZAK and F. M. KO, *Ceram. Bull.* **66** (1987) 353.
12. L. C. SAWYER, M. JAMIESON, D. BRIKOWSKI, M. I. HAIDER and R. T. CHEN, *J. Amer. Ceram. Soc.* **70** (1987) 798.
13. C. LAFFON, P. LAGARDE, A. M. FLANK, R. HAGEGE, P. OLRY, J. COTTERET, S. DIXMIER, M. LARIDJANI, A. P. LEGRAND and B. HOMELLE, *J. Mater. Sci.* **24** (1989) 1503.
14. Y. HASEGAWA and K. OKAMURA, *ibid.* **18** (1983) 3633.
15. S. YAJIMA, Y. HASEGAWA, J. HAYASHI and M. IIMURA, *ibid.* **13** (1978) 2569.
16. Y. HASEGAWA and K. OKAMURA, *ibid.* **21** (1986) 321.
17. J. C. SARTHOU, *University th*esis 155, Bordeaux (1984).
18. J. J. POUPEAU, D. ABBE and J. JAMET, ONERA Report (1982).
19. L. PORTE and A. SARTRE, *J. Mater. Sci.* **24** (1989) 271.
20. Y. MISOKAWA, K. M. GEIB and C. W. WINSEM, *J. Vac. Sci. Technol. A* **4** (1986) 1696.
21. J. LIPOWITZ, H. A. FREEMAN, R. T. CHEN and E. R. PRACK, *Adv. Ceram. Mater.* **2** (1987) 121.
22. D. BOUCHIER and A. BOSSEBOEUF, *Thin Solid Films* **139** (1986) 95.
23. P. LESPADE, A. MARCHAND, M. COUZI and F. CRUEGE, *Carbon* **22** (1984) 375.
24. F. TUINSTRA and J. L. KOENIG, *J. Chem. Phys.* **53** (1970) 1126.
25. B. S. ELMAN, M. S. DRESSELHAUS, G. DRESSELHAUS, E. W. MABY and H. MAZUREK, *Phys. Rev. B* **24** (1981) 1027.
26. T. C. CHIEU, M. S. DRESSELHAUS and M. ENDO, *ibid.* **26** (1982) 5867.
27. M. GORMAN and S. A. SOLIN, *Solid State Commun.* **15** (1974) 761,
28. Y. INOUE, S. NAKASHIMA, A. MITSUISHI, S. TABATA and S. TSUBOI, *ibid.* **48** (1983) 1071.
29. A. MORIMOTO, T. KATAOKA, M. KUMEDA and T. SHIMIZU, *Philos. Mag. B* **50** (1984) 517.
30. P. MARTINEAU, M. LAHAYE, R. PAILLER, R. NASLAIN, M. COUZI and F. CRUEGE, *J. Mater. Sci.* **19** (1984) 2731.
31. M. MONTHIOUX, A. OBERLIN and E. BOUILLON, *Compos. Sci. Technol.* **37** (1990) 21.
32. H. A. POHL, in "Modern Aspects of the Vitrous State", Vol. 2, edited by J. D. Mackenzie (London, 1972) p. 72.
33. M. RODOT, "Les Matériaux Semi Conducteurs", Vol. 2 (Dunod, Paris, 1965).
34. F. CARMONA, P. DELHAES, F. BARREAU, D. ORDIERA, R. CANET and L. LAFEYCHINE, *J. Phys.* **41** (1980) 531.
35. S. M. JOHNSON, R. D. BRITTAIN, R. H. LAMOREAUX and D. J. RAWCLIFFE, *J. Amer. Ceram. Soc.* **71** (1988) C-132.

Received 26 May
and accepted 23 October 1989